Estimating Thermal Conductivity of Frozen Soils from Air-filled Porosity

Zhengchao Tian[1&2]*, Tusheng Ren[3], Joshua L. Heitman[4], Robert Horton[5]

[1] College of Resources and Environment, Huazhong Agricultural University, Wuhan, 430070, China

[2] Key Laboratory of Arable Land Conservation (Middle and Lower Reaches of Yangtze River), Ministry of Agriculture and Rural Affairs, Wuhan, 430070, China

[3] College of Land Science and Technology, China Agricultural University, Beijing, 100193, China

[4] Department of Crop & Soil Sciences, North Carolina State University, Raleigh, NC, 27695, USA

[5] Department of Agronomy, Iowa State University, Ames, IA, 50011, USA

* Corresponding author: tianzhengchao@mail.hzau.edu.cn

This article has been accepted for publication and undergone full peer review but has not been through the copyediting, typesetting, pagination and proofreading process, which may lead to differences between this version and the Version of Record. Please cite this article as doi: 10.1002/saj2.20102.

ABSTRACT

Soil thermal conductivity (λ) is an important thermal property for environmental, agricultural, and engineering heat transfer applications. Existing λ models for frozen soils are complicated to use because they require estimates of both liquid water content and ice content. This study introduces a new approach to estimate λ of partially frozen soils from air-filled porosity (n_a), which can be determined by using an oven-drying method. A λ and n_a relationship was established based on measurements for 28 partially frozen soils. A strong exponential relationship between λ and n_a was found (with R^2 of 0.82). Independent tests on 10 partially frozen soils showed that the exponential λ-n_a model produced reliable λ estimates with a RMSE of 0.319 W m^{-1} K^{-1}, which was smaller than those of two widely used λ models for partially frozen soils. The λ-n_a model is easier to use than existing models, because it requires fewer parameters. Note that the λ-n_a model ignores the effect of temperature on λ of frozen soils and is most applicable to soil at temperatures ≤ -4°C.

Abbreviations: TDR, time domain reflectometry; SE, standard error of the regression; RMSE, root mean square error.

Soil thermal conductivity (λ) is a key parameter in modeling heat transfer in the vadose zone, which is important for environmental science, ground engineering, and geothermal applications (Dai et al., 2019). Direct measurement of λ can be time-consuming and somewhat difficult, especially for frozen soils (Tian et al., 2016). Substantial effort has been devoted to developing empirical or semi-theoretical models that estimate λ from basic soil properties (de Vries, 1963; Côté and Konrad, 2005; Lu et al., 2007; Lu et al., 2014). For frozen soils, the de Vries- and Johansen-based λ models have been widely used (Penner et al., 1975; Johansen, 1975; Tian et al., 2016). When soil freezes, there exists unfrozen liquid water in the soil pores, i.e., remaining partially frozen, due to the absorptive and capillary forces exerted by soil particles. The de Vries-based models give reliable λ estimates for partially frozen soils, but they require accurate liquid water content (θ_w) and ice content (θ_i) values, which are difficult to measure. The Johansen-based models estimate λ of partially frozen soils from λ values of dry soils and saturated frozen soils at the same bulk density (ρ_b), which also requires θ_w and θ_i values at saturation. Although several techniques have been tested for measuring θ_w and θ_i in partially frozen soils, the accuracy of these techniques is questionable, because no independent verification method is available (Watanabe and Wake, 2009; Zhou et al., 2014; Tian et al., 2019; Kojima et al., 2020). Thus, it is necessary to develop models that estimate λ of partially frozen soils using more easily measurable parameters.

Previous studies reported that λ values of unfrozen and frozen soils are greatly affected by soil water (θ_w and θ_i) and ρ_b conditions, and the correlations between λ and θ_w, θ_i, and ρ_b vary significantly among soil types (Abu-Hamdeh and Reeder, 2000; Côté and Konrad, 2005). Ochsner et al. (2000), however, observed that the air-filled porosity (n_a), rather than θ_w and ρ_b, had a dominant effect on λ of unfrozen soils. Xie et al. (2019) showed that, for unfrozen soils, the λ and n_a relationship could be approximated using a general linear function. For partially frozen soils, the n_a is approximated by the difference between soil porosity (η) and total water content (θ_{tot}) because liquid water and ice have fairly similar densities (about 1 and 0.92 Mg m^{-3}, respectively), which differ substantially from that of the soil solid phase (about 2.65 Mg m^{-3} for many mineral soils). Considering the fact that η and θ_{tot} in mineral soils can be measured easily and accurately with the oven-drying method, it is common for η and θ_{tot} to be used as independent variables in λ models. To the best of our knowledge, no studies have reported the influences of n_a on λ of partially frozen soils, nor whether λ of partially frozen soils can be estimated directly from n_a measurements.

The objectives of this research are to examine the relationship between n_a and λ for partially frozen soils and to develop a single-parameter model that estimates λ from n_a. Literature λ data for 28 partially frozen soils with various textures at different θ_{tot} and ρ_b values are used to develop the λ-n_a model. Independent data from another 10 soils are used to evaluate the accuracy of the new model.

MATERIALS AND METHODS

Thermal Conductivity Dataset of Partially Frozen Soils

Due to the difficulties in accurately determining λ of partially frozen soils, a limited number of datasets are available in the literature. In this work, λ measurements on 38 partially frozen soils were obtained from Kersten (1949), Penner et al. (1970, 1975), Inaba (1983), Jacobs and Perkins (1990), and Tian et al. (2016, 2017). The λ values for 10 soils from Kersten (1949) and four soils from Jacobs and Perkins (1990) were determined with the steady state method at a mean temperature of -4^{o}C. The λ values for 10 soils from Penner et al. (1970, 1975) and three soils from Inaba (1983) were measured with a single-probe heat-pulse method at temperatures from -2^{o}C to -20^{o}C. The λ data for 11 soils from Tian et al. (2016, 2017) were determined with the dual-probe heat-pulse method at temperatures from -1 to -15^{o}C. Because the heat-pulse method performed poorly at temperatures from 0 to -5^{o}C (Tian et al., 2015), only the heat-pulse measurements at temperatures ≤ -5^{o}C were used in this study. Table 1 presents the basic physical properties of the investigated soils. The 38 soils were grouped into two datasets: Soils 1-28 with a total of 229 measurements were used to establish the relationship between λ and n_a, and Soils 29-38 with a total of 111 measurements were used to examine the accuracy of the λ-n_a model. The 38 soils were classified into model-fitting and validation groups based on two principles: (1) Both groups included a wide range of soil texture, ρ_b, and θ_{tot}; (2) Both groups contained λ measurements from three different methods (Table 1). Figure 1 shows the textural class distribution of the datasets according to the USDA system. Note that most of the investigated soils had organic carbon content less than 5%, and thus organic soils, such as peat, were not considered in this study.

Soil n_a values were calculated with the following equation,

$$n_a = 1 - v_s - \theta_w - \theta_i \approx 1 - v_s - \theta_{tot} \quad [1]$$

where $v_s = \rho_b/\rho_s$ is the volume fraction of soil solids and ρ_s is soil particle density. ρ_s is assumed herein to be 2.65 Mg m^{-3} when it is not otherwise reported (Hillel, 2004).

We examined the relationships between λ and θ_{tot}, v_s, and n_a. The significance of these relationships was assessed with the coefficient of determination (R^2) and the standard error of the regression (SE).

Thermal Conductivity Models for Partially Frozen Soils

In this study, we assumed that for partially frozen soils, a linear or nonlinear empirical relationship existed between λ and n_a, and the relationship could be used to estimate λ from n_a measurements. The λ-n_a model was developed using data for the 28 soils in the model-fitting dataset. The performance of the λ-n_a model was evaluated with data for the 10 soils in the validation dataset and by comparing its performance versus the de Vries- and Johansen-based λ models.

The de Vries-based λ model for partially frozen soils is (Tian et al., 2016),

$$\lambda = \frac{\theta_w\lambda_w + k_i\theta_i\lambda_i + k_a n_a\lambda_a + k_s v_s\lambda_s}{\theta_w + k_i\theta_i + k_a n_a + k_s v_s} \qquad [2]$$

where λ_w (0.57 W m^{-1} K^{-1}), λ_i (2.28 W m^{-1} K^{-1}), λ_a (0.024 W m^{-1} K^{-1}), and λ_s represent thermal conductivities of liquid water, ice, air, and soil solids, respectively; and k_i, k_a, and k_s are weighting factors for ice, air, and soil solids, respectively. The parameter λ_s is estimated from soil texture information with (Tian et al., 2016),

$$\lambda_s = \lambda_{sand}{}^{f_{sand}}\lambda_{silt}{}^{f_{silt}}\lambda_{clay}{}^{f_{clay}} \qquad [3]$$

where λ_{sand} (7.70 W m^{-1} K^{-1}), λ_{silt} (2.74 W m^{-1} K^{-1}), and λ_{clay} (1.93 W m^{-1} K^{-1}) are thermal conductivities of sand, silt, and clay, respectively; and f_{sand}, f_{silt}, and f_{clay} are the volume fractions of sand, silt, and clay in soil solids, respectively.

The weighting factor k_j in Eq. [2] is:

$$k_j = \frac{2}{3}\left[1 + \left(\frac{\lambda_j}{\lambda_w} - 1\right) g_{a(j)}\right]^{-1} + \frac{1}{3}\left[1 + \left(\frac{\lambda_j}{\lambda_w} - 1\right)(1 - 2g_{a(j)})\right]^{-1} \qquad [4]$$

where the subscript j represents ice, air, and soil solids; and $g_{a(j)}$ is the shape factor for ice crystals, solid particles, and air voids. The shape factor $g_{a(j)}$ is given by,

$$g_{\mathrm{a(ice)}} = 0.333\left(1 - \frac{\theta_\mathrm{i}}{1-v_\mathrm{s}}\right) \quad [5]$$

$$g_{\mathrm{a(air)}} = 0.333\left(1 - \frac{n_\mathrm{a}}{1-v_\mathrm{s}}\right) \quad [6]$$

$$g_{\mathrm{a(solids)}} = g_{\mathrm{a(sand)}}f_{\mathrm{sand}} + g_{\mathrm{a(silt)}}f_{\mathrm{silt}} + g_{\mathrm{a(clay)}}f_{\mathrm{clay}} \quad [7]$$

where $g_{\mathrm{a(sand)}}$, $g_{\mathrm{a(silt)}}$, and $g_{\mathrm{a(clay)}}$ are 0.182, 0.0534, and 0.00775, respectively (Tian et al., 2016). Note that, Eq. [2] treats liquid water as a continuous phase in partially frozen soils, which might be inappropriate at a sufficiently low temperature when ice becomes the continuous phase. The λ of soils used in this study were measured at temperatures ≥ -20°C, and thus, for simplicity, we treated water as a continuous phase for all samples.

The Johansen-based model is (Johansen, 1975; Lu et al., 2007),

$$\lambda = \left(\lambda_{\mathrm{sat}} - \lambda_{\mathrm{dry}}\right)K_\mathrm{e} + \lambda_{\mathrm{dry}} \quad [8]$$

where λ_{sat} and λ_{dry} are λ values for saturated frozen and dry soils, respectively; and K_e is the normalized thermal conductivity which is equal to the degree of saturation (S_e) in partially frozen soils. λ_{sat} , λ_{dry}, and S_e are as follows,

$$\lambda_{\mathrm{sat}} = {\lambda_\mathrm{s}}^{v_\mathrm{s}}{\lambda_\mathrm{w}}^{\theta_{\mathrm{w(sat)}}}{\lambda_\mathrm{i}}^{\left[1-v_\mathrm{s}-\theta_{\mathrm{w(sat)}}\right]} \quad [9]$$

$$\lambda_{\mathrm{dry}} = -0.56(1 - v_\mathrm{s}) + 0.51 \quad [10]$$

$$S_\mathrm{e} = \frac{\theta_\mathrm{w}+\theta_\mathrm{i}}{1-v_\mathrm{s}} \quad [11]$$

where λ_s is obtained with Eq. [3], and $\theta_{w(sat)}$ is the θ_w value of the partially frozen soil sample at saturation.

Both the de Vries- and Johansen-based λ models require θ_w and θ_i estimates and soil texture information. For the soils from Tian et al. (2016, 2017), θ_w values were measured with the TDR technique, and θ_i values were obtained from the difference between θ_{tot} and θ_w (i.e., $\theta_i = (\theta_{tot} - \theta_w)\rho_w/\rho_i$, where ρ_w and ρ_i are densities of water and ice, respectively). For the soils from Inaba (1983), θ_w values were determined by a calorimetric technique. For the soils from Kersten (1949) and Penner et al. (1975), θ_w values were not available, and thus, were estimated from soil freezing characteristic curves. Please refer to Tian et al. (2016) for details on how to estimate θ_w from soil freezing characteristic curves. For soil particle size analysis, Tian et al. (2016, 2017) used the pipette method, and Kersten (1949), Penner et al. (1975), and Inaba (1983) used the hydrometer and sieve methods. The root mean square error (RMSE) and R^2 values between the measured and estimated λ values were calculated to evaluate performances of the λ models.

RESULTS AND DISCUSSION

Although the effects of θ_{tot}, v_s, ρ_b, salt concentration, and organic matter content on λ of unfrozen and partially frozen soils have been investigated (Abu-Hamdeh and Reeder, 2000; Mustamo et al., 2019; Zhao and Si, 2019), no universal relationship has been established between λ and these variables. Alternately, in unfrozen soils, λ has been observed to exhibit a general linear correlation with n_a across a wide range of textures (Ochsner et al., 2000; Tong et al., 2019; Xie et al., 2019). Figure 2 illustrates λ as a function of θ_{tot}, v_s, or n_a for 28 partially frozen soils. Similar to that for unfrozen soils, only a moderate linear relationship was observed between λ and θ_{tot} with an R^2 of 0.44 and an SE of 0.634 W m^{-1} K^{-1} (Fig. 2a), which indicated that λ somewhat depended on θ_{tot} in partially frozen soils. However, such a linear function was inadequate to model λ of partially frozen soils. Although the λ of partially frozen soils also increased with v_s, the correlation between λ and v_s was weak as the R^2 was 0.14 and the SE value was 0.785 W m^{-1} K^{-1} (Fig. 2b).

In unfrozen soils, n_a (rather than θ_w or v_s) is a key factor that impacts λ, because λ of air (0.025 W m^{-1} K^{-1} at 20^{o}C) is much lower than that of water and soil solids (0.60 and ~3.5 W m^{-1} K^{-1} at 20^{o}C, respectively). Likewise, in partially frozen soils, n_a may manifest a simpler direct relationship with λ than do liquid water, ice (with a λ of 2.28 W m^{-1} K^{-1}), or v_s. In this study, we observed strong linear and exponential relationships between λ and n_a on 28 partially frozen soils (Fig. 2c). The fitted linear equation had an R^2 of 0.74 and an SE of 0.428 W m^{-1} K^{-1}. The fitted exponential equation between λ and n_a for the 28 soils had an R^2 of 0.82 and an SE of 0.368 W m^{-1} K^{-1}. Additionally, the exponential λ-n_a model avoids negative λ estimates at large n_a values. The following gives the exponential λ-n_a fitting equation,

$$\lambda = 3.14e^{-4.92n_a} \quad [12]$$

The R^2 of Equation [12] was much greater than that of the λ-θ_{tot} and the λ-v_s functions, and the SE of Eq. [12] was less than half that of the λ-θ_{tot} and the λ-v_s functions. Thus, the exponential function explained much of the variation in λ and could be an appropriate model to estimate λ of partially frozen soils.

Figure 3a presents the comparison between Eq. [12] estimated λ values and measured λ values of the 10 partially frozen soils in the validation dataset. In general, the data distributed randomly along the 1:1 line with a RMSE of 0.319 W m^{-1} K^{-1}. The R^2 of the fitted linear relation between estimated and measured λ values was 0.85. The performance of the de Vries-based and the Johansen-based λ models on the same soils were also evaluated in this study (Figs. 3b and 3c). The de Vries-based model gave reasonable λ estimates for the 10 partially frozen soils with a RMSE of 0.370 W m^{-1} K^{-1} and an R^2 of 0.83. The Johansen-based model had a RMSE of 0.376 W m^{-1} K^{-1} and R^2 of 0.80. Thus, the exponential λ-n_a model could give λ estimates as accurate as or even slightly better than the de Vries- and Johansen-based models. More importantly, unlike the de Vries-based and the Johansen-based models, the exponential λ-n_a model is simple to use and has a practical advantage, because it does not require soil texture, θ_w, and θ_i measurements.

It is worth noting that the exponential λ-n_a model ignores the effect of temperature on λ of partially frozen soils, because the measurements of both the model-fitting and validation datasets are mostly carried out at temperatures $\leq$ -4°C at which the λ varies little with temperatures (Inaba, 1983). The effect of temperature on λ of frozen soils can be significant at temperatures close to 0°C (Zhao and Si, 2019). However, only a few λ measurements at such temperatures are available in the literature, because it is quite difficult for the steady state and the heat-pulse methods to determine λ of partially frozen soils at temperatures near 0°C. Fig. 4 shows the performance of three models on estimating λ of partially frozen soils at temperatures of -1 and -2°C using a limited number of measured values from Inaba (1983) and Tian et al. (2017). Among the three models, the de Vries-based model provides the most accurate λ estimates with a RMSE of 0.319 W m^{-1} K^{-1}. The exponential λ-n_a model and the Johansen-based model have RMSE values of 0.349 and 0.340 W m^{-1} K^{-1}, respectively. The exponential λ-n_a model may perform worse at temperatures between -1 to 0°C as a large phase change of water occurs with temperature changes under such a condition. Besides, the measurement accuracy of the steady-state and transient methods is also questionable during this temperature range due to the significant latent heat effect on the measurement. Thus, the exponential λ-n_a model is most applicable to soils at temperatures ≤ -4°C.

CONCLUSIONS

In this note, we examined the effects of θ_{tot}, v_s, and n_a on λ of partially frozen soils. A strong exponential relationship was found between λ and n_a across a wide range of soils. The exponential λ-n_a function gave reliable λ estimates for the partially frozen soils at temperatures ≤ -4°C with a RMSE of 0.319 W m^{-1} K^{-1}. The accuracy of the new model was greater than the widely used de Vries- and Johansen-based models, which had RMSE values ≥ 0.370 W m^{-1} K^{-1}. In addition, the new model did not require specific information about soil texture nor separate estimates of ice and liquid water contents. Thus, we conclude that the new single parameter n_a model can estimate λ of partially frozen soils at temperatures ≤ -4°C with satisfactory accuracy.

ACKNOWLEDGEMENTS

This work is supported by the National Natural Science Foundation of China (41907003), the China Fundamental Research Funds for the Central Universities (No. 2662019QD014), the U.S. Army Research Office (W911NF-16-1-0287), and the U.S. National Science

Foundation (1623806), and the USDA-NIFA multi-State Project 4188, by Hatch Act, and State of Iowa.

REFERENCES

Abu-Hamdeh, N.H., and R.C. Reeder. 2000. Soil thermal conductivity effects of density, moisture, salt concentration, and organic matter. Soil Sci. Soc. Am. J. 64(4): 1285–1290.

Côté, J., and J.M. Konrad. 2005. A generalized thermal conductivity model for soils and construction materials. Can. Geotech. J. 42(2): 443–458.

Dai, Y., N. Wei, H. Yuan, S. Zhang, W. Shangguan, S. Liu, X. Lu, and Y. Xin. 2019. Evaluation of soil thermal conductivity schemes for use in land surface modeling. J. Adv. Model. Earth Sy. 11: 3454–3473.

de Vries, D.A. 1963. Thermal properties of soils. In: Van Wijk, W.R. (Ed.), Physics of Plant Environment, pp. 210–235. North-Holland Pub. Co., Amsterdam, the Netherlands.

Hillel, D. 2004. Introduction to Environmental Soil Physics. Elsevier Academic Press, Amsterdam, the Netherlands.

Inaba, H. 1983. Experimental study on thermal properties of frozen soils. Cold Reg. Sci. Technol. 8(2): 181–187.

Jacobs, H.R., and F.M. Perkins. 1990. Determination of thermal conductivity in freezing moist soils. Exp. Therm. Fluid Sci. 3(4): 355–361.

Johansen, O. 1975. Thermal conductivity of soils. PhD thesis, Norwegian University of Science and Technology, Trondheim, Norway.

Kersten, M.S. 1949. Thermal properties of soils. University of Minnesota, Eng. Exp. Sta. Bull. No. 28, Minneapolis, MN.

Kojima, Y., Y. Nakano, C. Kato, K. Noborio, K. Kamiya, and R. Horton. 2020. A new thermo-time domain reflectometry approach to quantify soil ice content at temperatures near the freezing point. Cold Reg. Sci. Technol. 174: 103060.

Lu, S., T. Ren, Y. Gong, and R. Horton. 2007. An improved model for predicting soil thermal conductivity from water content at room temperature. Soil Sci. Soc. Am. J. 71(1): 8–14.

Lu, Y., S. Lu, R. Horton, R., and T. Ren. 2014. An empirical model for estimating soil thermal conductivity from texture, water content, and bulk density. Soil Sci. Soc. Am. J. 78(6): 1859–1868.

Mustamo, P., A.K. Ronkanen, Ö. Berglund, K. Berglund, and B. Kløve. 2019. Thermal conductivity of unfrozen and partially frozen managed peat soils. Soil Till. Res. 191: 245–255.

Ochsner, T.E., R. Horton, and T. Ren. 2001. A new perspective on soil thermal properties. Soil Sci. Soc. Am. J. 65(6): 1641–1647.

Penner, E. 1970. Thermal conductivity of frozen soils. Can. J. Earth Sci. 7: 982–987.

Penner, E., G.H. Johnston, and L.E. Goodrich. 1975. Thermal conductivity laboratory studies of some Mackenzie Highway soils. Can. Geotech. J. 12: 271–288.

Tian, Z., J. Heitman, R. Horton, and T. Ren, T. 2015. Determining soil ice contents during freezing and thawing with thermo-time domain reflectometry. Vadose Zone J. 14(8).

Tian, Z., Y. Lu, R. Horton, and T. Ren. 2016. A simplified de Vries–based model to estimate thermal conductivity of unfrozen and frozen soil. Eur. J. Soil Sci. 67(5): 564–572.

Tian, Z., T. Ren, Y. Kojima, Y. Lu, R. Horton, and J.L. Heitman. 2017. An improved thermo time domain reflectometry method for determination of ice contents in partially frozen soils. J. Hydrol. 555: 786–796.

Tian, Z., Y. Kojima, J.L. Heitman, R. Horton, and T. Ren. 2019. Advances in thermo-time domain reflectometry technique: measuring ice content in partially frozen soils. Methods of Soil Analysis. 4(1): 190003.

Tong, B., D. Kool, J.L. Heitman, T.J. Sauer, Z. Gao, and R. Horton. 2019. Thermal property values of a central Iowa soil as functions of soil water content and bulk density or of soil air content. Eur. J. Soil Sci. doi: 10.1111/ejss.12856

Watanabe, K., and T. Wake. 2009. Measurement of unfrozen water content and relative permittivity of frozen unsaturated soil using NMR and TDR. Cold Reg. Sci. Technol. 59(1): 34–41.

Xie, X., Y. Lu, T. Ren, and R. Horton. 2019. Thermal conductivity of mineral soils relates linearly to air-filled porosity. Soil Sci. Soc. Am. J. doi: 10.1002/saj2.20016.

Zhao, Y., and B. Si. 2019. Thermal properties of sandy and peat soils under unfrozen and frozen conditions. Soil Till. Res. 189: 64–72.

Zhou, X., J. Zhou, W. Kinzelbach, and F. Stauffer. 2014. Simultaneous measurement of unfrozen water content and ice content in frozen soil using gamma ray attenuation and TDR. Water Resour. Res. 50(12): 9630–9655.

List of figure captions:

Fig. 1. Textural distribution of the partially-frozen soils for the model-fitting and validation datasets. Note, texture information for soils from Jacobs and Perkins (1990) was not reported, and thus, is not included here.

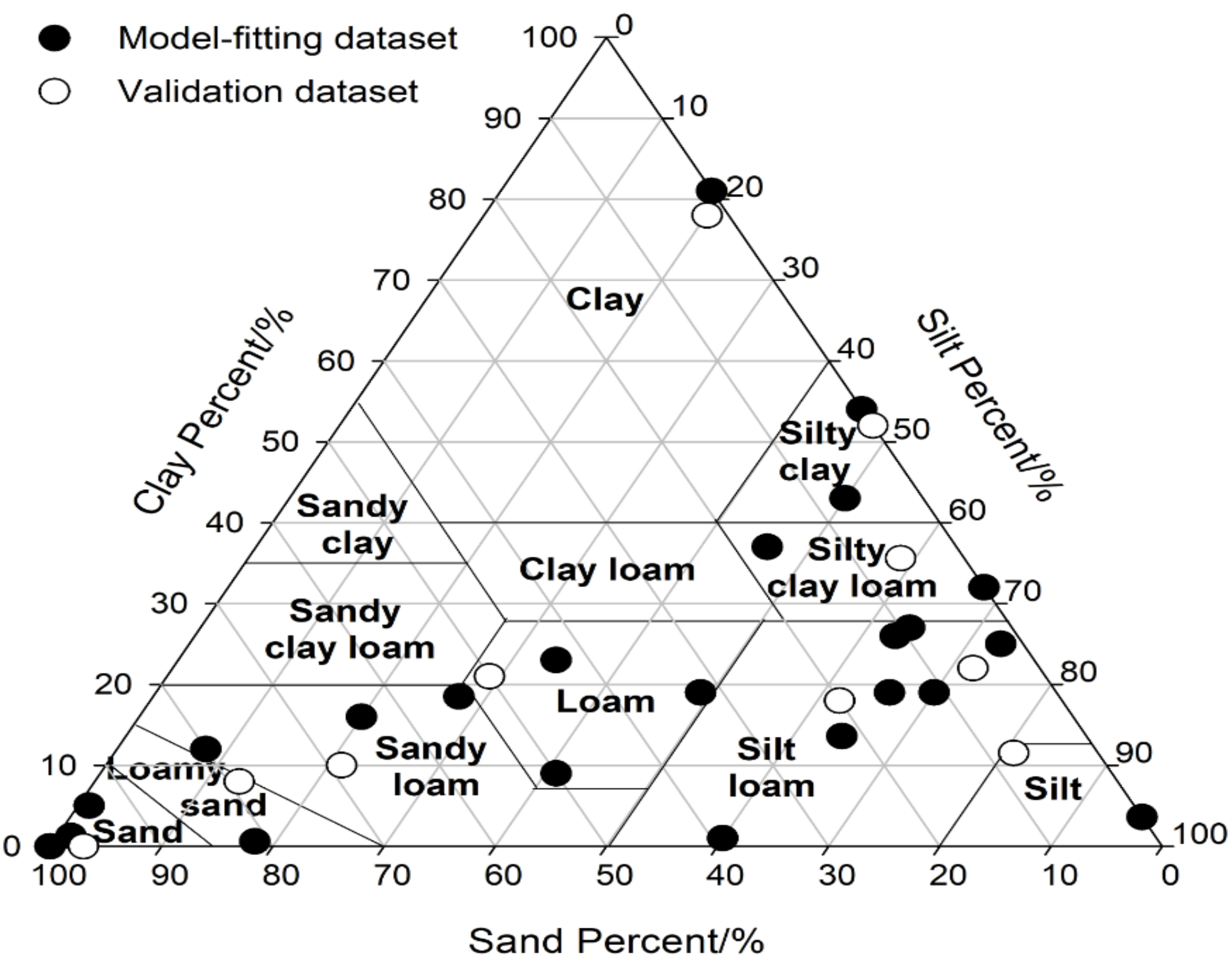

Fig. 2. Soil thermal conductivity (λ) as functions of (a) total water content (θ_{tot}), (b) volume fraction of soil solids (v_s), and (c) air-filled porosity (n_a) for 28 partially-frozen soils in the model-fitting dataset. Dashed and solid lines represent the fitted regression functions.

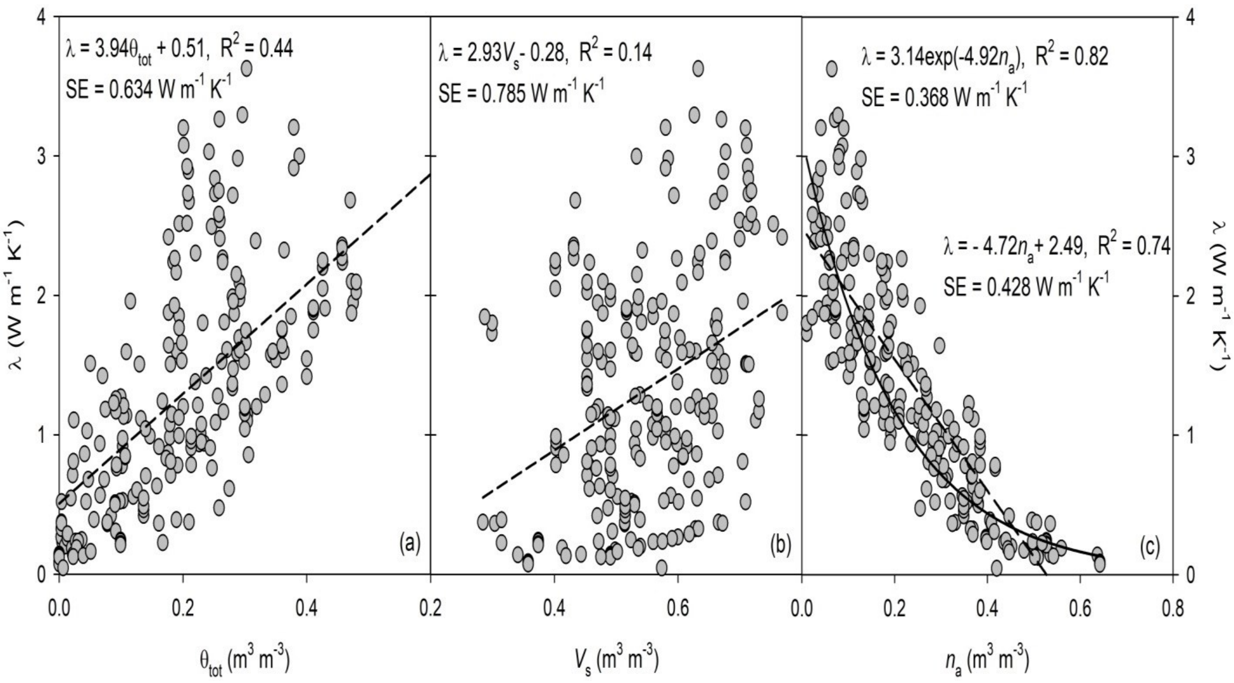

Fig. 3. Comparison of estimated soil thermal conductivity (λ) vs. measured λ values for the (a) exponential model of air-filled porosity (n_a), the (b) de Vries-based model, and the (c) Johansen-based model for the 10 partially-frozen soils of the validation dataset. Solid lines are the 1:1 lines, and dashed lines are linear regressions.

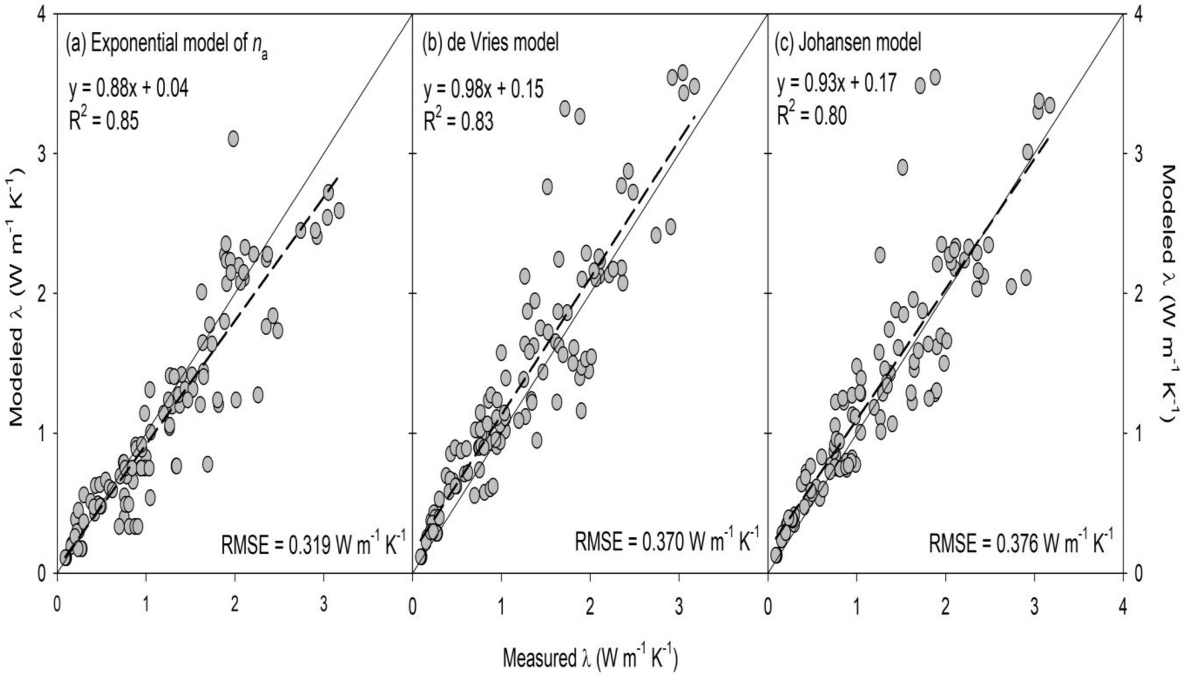

Fig. 4. Comparison of estimated soil thermal conductivity (λ) vs. measured λ values for the (a) exponential model of air-filled porosity (n_a), the (b) de Vries-based model, and the (c) Johansen-based model for the partially-frozen soils measured at temperatures of -1 and -2°C. Solid lines are the 1:1 lines, and dashed lines are linear regressions.

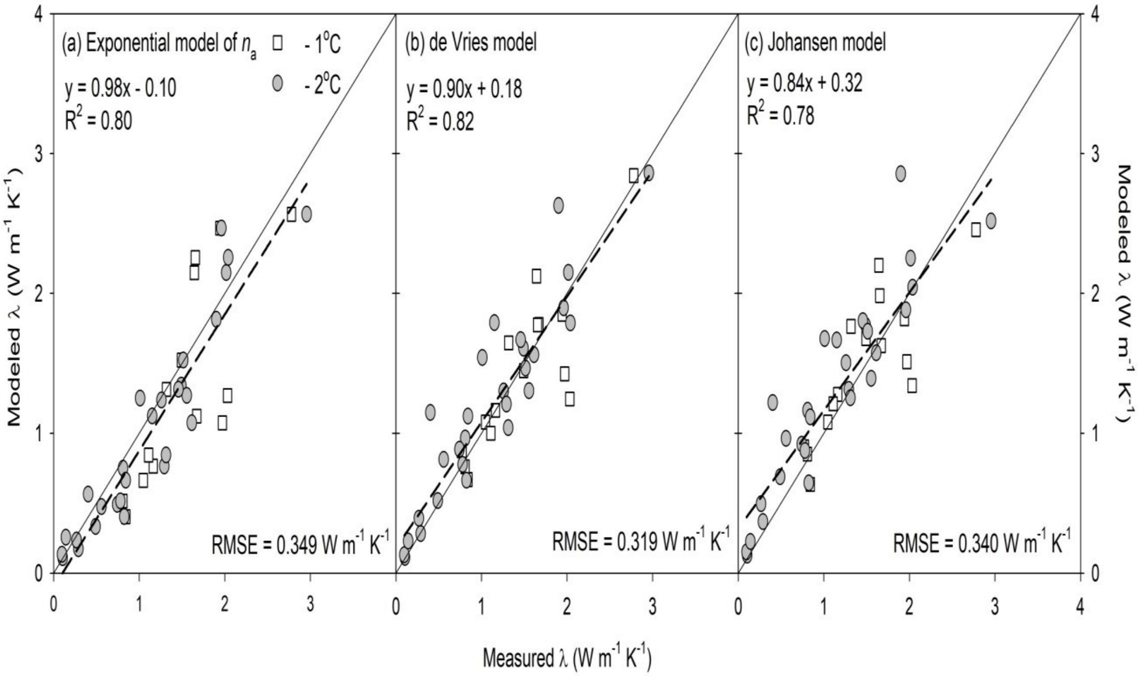

Table 1. Soil ID, particle-size distribution (PSD), texture, measurement temperature (T), particle density (ρ_s), bulk density (ρ_b), initial total water content (θ_{tot}), air-filled porosity (n_a), and measurement method of thermal conductivity of the frozen soils used in this study.

ID	PSD Sand	PSD Silt	PSD Clay	Texture	T	ρ_s	ρ_b	θ_{tot}	n_a	Method
	------------- % -------------				°C	Mg m^{-3}	Mg m^{-3}	m^3 m^{-3}	m^3 m^{-3}	
1	98	1	1	Sand	-4	2.72	1.71~1.97	0.00~0.30	0.06~0.37	SS
2	100	0	0	Sand	-4	2.67	1.49~1.90	0.00~0.30	0.08~0.44	SS
3	100	0	0	Sand	-4	2.74	1.48~1.81	0.01~0.34	0.09~0.45	SS
4	94	1	5	Sand	-10	2.65	1.46~1.59	0.09~0.29	0.13~0.36	DPHP
5	81	18	1	Loamy sand	-6 ~ -20	2.65	1.14~1.50	0.00~0.46	0.07~0.51	SPHP
6	80	8	12	Sandy loam	-5 ~ -15	2.65	1.30	0.16~0.47	0.10~0.35	DPHP
7	64	20	16	Sandy loam	-5, -15	2.70	1.66~1.89	0.10~0.25	0.03~0.25	SPHP

8	54	28	19	Sandy loam	-4	2.68	1.40~2.02	0.04~0.32	0.03~0.44	SS
9	50	41	9	Loam	-10	2.65	1.22~1.42	0.13~0.28	0.18~0.37	DPHP
10	43	34	23	Loam	-5, -15	2.70	1.94~2.07	0.09~0.26	0.02~0.18	SPHP
11	32	49	19	Loam	-5, -15	2.70	1.66~1.89	0.10~0.26	0.04~0.28	SPHP
12	39	60	1	Silt loam	-5, -10	2.65	1.24~1.54	0.12~0.38	0.04~0.38	DPHP
13	22	64	14	Silt loam	-4	2.70	1.20~1.57	0.02~0.35	0.07~0.54	SS
14	11	63	26	Silt loam	-5, -15	2.70	1.64~1.83	0.11~0.26	0.06~0.29	SPHP
15	11	70	19	Silt loam	-10	2.65	1.26~1.41	0.14~0.39	0.08~0.37	DPHP
16	15	66	19	Silt loam	-5, -10	2.65	1.30	0.09~0.29	0.22~0.42	DPHP
17	2	73	25	Silt loam	-5, -10	2.65	1.20	0.18~0.48	0.07~0.37	DPHP
18	0	96	4	Silt	-6 ~	2.65	0.95~1.20	0.00~0.43	0.17~0.64	SPHP

					-20					
19	17	46	37	Silty clay loam	-5 ~ -15	2.65	1.30	0.13~0.46	0.09~0.38	DPHP
20	9	64	27	Silty clay loam	-4	2.71	0.92~1.63	0.02~0.47	0.04~0.64	SS
21	0	68	32	Silty clay loam	-5, -15	2.70	1.43~1.64	0.09~0.29	0.10~0.38	SPHP
22	7	50	43	Silty clay	-5, -10	2.65	1.20~1.43	0.09~0.47	0.05~0.42	DPHP
23	0	46	54	Silty clay	-5, -15	2.70	1.39~1.57	0.08~0.30	0.12~0.41	SPHP
24	0	19	81	Clay	-5 ~ -20	2.65	0.79	0.69	0.02	SPHP
25	N.A.	N.A.	N.A.	N.A.	-4	2.65	0.81~1.26	0.02~0.24	0.30~0.54	SS
26	N.A.	N.A.	N.A.	N.A.	-4	2.65	0.75~1.21	0.04~0.31	0.27~0.54	SS
27	N.A.	N.A.	N.A.	N.A.	-4	2.65	0.83~1.33	0.05~0.26	0.25~0.52	SS
28	N.A.	N.A.	N.A.	N.A.	-4	2.65	1.24~1.52	0.01~0.45	0.01~0.42	SS

29	97	3	0	Sand	-4	2.76	1.56~1.86	0.01~0.25	0.11~0.43	SS
30	79	13	8	Loamy sand	-10	2.65	1.22~1.42	0.08~0.28	0.18~0.42	DPHP
31	69	21	10	Sandy loam	-4	2.71	1.35~2.19	0.03~0.32	0.03~0.48	SS
32	50	29	21	loam	-5, -10	2.65	1.20	0.17~0.47	0.08~0.38	DPHP
33	20	62	18	Silt loam	-5, -15	2.70	1.61~1.79	0.10~0.29	0.05~0.31	SPHP
34	6	72	22	Silt loam	-5, -15	2.70	1.69~1.86	0.08~0.25	0.07~0.29	SPHP
35	8	81	11	Silt	-4	2.70	1.12~1.75	0.03~0.48	0.07~0.56	SS
36	6	59	35	Silty clay loam	-6 ~ -20	2.65	0.84~1.05	0.00~0.42	0.19~0.68	SPHP
37	0	48	52	Silty clay	-5, -15	2.70	1.40~1.63	0.10~0.33	0.07~0.38	SPHP
38	2	20	78	Clay	-4	2.59	1.03~1.73	0.03~0.44	0.00~0.57	SS

Note: N.A., not available; SS, steady state method; SPHP, single-probe heat-pulse method; DPHP, dual-probe heat-pulse method.